THE ASTROPHYSICAL JOURNAL, 183:819–841, 1973 August 1

NONLINEAR GASEOUS DENSITY WAVES AND GALACTIC SHOCKS

FRANK H. SHU* AND VINCENZO MILIONE†
State University of New York at Stony Brook
AND
WILLIAM W. ROBERTS, JR.
University of Virginia
Received 1972 October 30; revised 1973 March 9

ABSTRACT

We follow the perturbations in the flow of interstellar gas which result from steady forcing by spiral gravitational fields of various strengths. The density response is quite nonlinear even if the amplitude of the spiral field maintained by the disk stars is only a small fraction of the basic axisymmetric field. An analytical study of the properties of slightly nonlinear flows yields certain results which are qualitatively similar to those found numerically for fully nonlinear flows. Galactic shocks arise naturally, indeed *necessarily*, if the strength of the underlying spiral gravitational field exceeds a certain critical value.

The breadth of the zone of high gas compression depends critically on whether the Doppler-shifted phase-velocity of the stellar density wave is greater than or less than the "effective acoustic speed" of the gas. In the former case, very narrow compression zones result; in the latter, quite broad zones. This distinction may explain why some galaxies have narrow optical arms while others have broad optical arms.

In addition, a certain range of values for the intrinsic frequency of the wave gives rise to ultra-harmonic resonances which can introduce secondary compressions of the interstellar gas. This result may relate directly to the origin of the Carina spiral feature in our own Galaxy as well as to the phenomena of branches, spurs, and feathers which are often seen in external spiral galaxies.

Subject headings: galactic structure — interstellar matter

I. INTRODUCTION

Nonlinear solutions for the large-scale flow of interstellar gas in the presence of a spiral gravitational field have recently received considerable theoretical attention (Fujimoto 1966; Roberts 1969*a*; Roberts and Yuan 1970; Vandervoort 1971; Shu *et al.* 1972; see also Mathewson, van der Kruit, and Brouw 1972 and Roberts 1972 for observations which bear on the galactic shock phenomenon in M51 and in the Perseus arm region of our own Galaxy). In this paper we wish to fill some important gaps left by the previous investigations: (1) What is the relation between flow solutions which contain shocks and those which do not? (2) What conditions must be fulfilled in a normal spiral galaxy for the zone of high gas compression (and, presumably, the zone of active star formation) to be very narrow? To be quite broad? (3) Can nonlinear effects account for *some* of the secondary arms, spurs, and feathers often seen in external galaxies?

Question 1 is relevant because Vandervoort (1971) has found nonlinear gaseous density waves which do not contain shocks. Thus, do the galactic shocks in the solutions given by Roberts (1969*a*) and by others, exist as a postulate additional to the usual assumptions of the density-wave theory (cf. Piddington 1973), or do they occur as a *necessary* consequence of the theory for waves of sufficiently large amplitudes?

* Alfred P. Sloan Foundation Fellow.
† Present address: Department of Civil Engineering, State University of New York, Buffalo.

Question 2 is significant because the motivation to search for flow solutions containing shocks arose originally to meet the challenge posed by galaxies with remarkably thin spiral arms—galaxies such as NGC 5364 which has H II regions lined up as "beads on a string." However, a complete theory must also be able to accommodate the galaxies with broad optical arms—galaxies such as M33. Thus, do the wave amplitudes in galaxies with broad arms not reach sufficiently large values to produce galactic shocks, or are the zones of high gas compression in such galaxies broad *despite the production of shocks*?

Question 3 is important because in many galaxies, bits and pieces of spiral features *coexist* with a "grand design" of spiral structure (see Lin 1971; cf. Piddington 1973). It is natural to associate these bits and pieces with sheared material arms whose origin lies with the local gravitational instability of the interstellar gas (Goldreich and Lynden-Bell 1965; Julian and Toomre 1966). But could *some* of these features also be associated with the nonlinear response of the gas to forcing by an *ordered* spiral gravitational field?

This paper, then, attempts to examine the above issues with a survey of the nonlinear phenomena which may have an important qualitative effect on the compressional history of the interstellar gas. Our first task is, thus, to review why the basic equations demand that the density response of the interstellar gas be generally quite nonlinear even if the amplitude of the spiral gravitational field is only a small fraction of the basic axisymmetric gravitational field.

II. BASIC EQUATIONS AND CONCEPTS

Before we begin the theoretical development, we shall recapitulate the fundamental equations and concepts. Our calculations concern the nonlinear response of the interstellar gas subjected to forcing by an imposed spiral gravitational field which is assumed to be supported primarily by the disk stars. The gravitational potential in the central plane of the galactic disk is assumed to be given by the linear theory, and, thus, to have the following form when written in polar coordinates $(\varpi, \phi = \theta - \Omega_p t)$ which rotate with the pattern speed $\Omega_p = \omega/m$:

$$\mathfrak{V} = \mathfrak{V}_0(\varpi) + A(\varpi) \cos \chi \,. \tag{1}$$

In the above equation, $\mathfrak{V}_0(\varpi)$ is the unperturbed axisymmetric potential; $A(\varpi)$ is the amplitude of the perturbation spiral potential; and χ is the phase function

$$\chi = \Phi(\varpi) - m\phi \,. \tag{2}$$

The integer m equals 2 for two-armed spirals.

For tightly wrapped spiral waves, $\Phi(\varpi)$ is a rapidly varying function and $A(\varpi)$ is a slowly varying function. In this asymptotic approximation, equipotential curves for the spiral gravitational potential are given by the lines of constant phase: χ = constant.

For most purposes the linear theory is adequate for the dynamics of the disk stars. However, because the response of a particular component of the galaxy to a given spiral field is roughly proportional to the inverse square of the relevant dispersive speed, the density response of the interstellar gas can be fully nonlinear even if the perturbation density of the disk stars amounts to only a few percent of the unperturbed value.

In the analysis of this paper, we follow Roberts (1969*a*) and adopt an isothermal one-component model of the interstellar medium characterized by a uniform "effective speed of sound," $a = 8$ km s^{-1}. This model provides an adequate description as long

as we limit ourselves to the discussion of phenomena with characteristic length scales larger than, say, 10^2 pc.[1]

In the linear theory of density waves, all perturbation quantities which arise in response to forcing by the potential (1) are found to vary much more rapidly in the direction perpendicular to the equipotential curves than in the direction along them. Assuming a similar behavior for the forced nonlinear density waves in the gaseous component, we are motivated to introduce the curvilinear coordinate system ($\eta = -\chi + \pi$, ξ) defined so that

$$d\eta = -kd\varpi + md\phi\,, \qquad d\xi = -m\frac{d\varpi}{\varpi} - k\varpi d\phi\,, \tag{3}$$

where the radial wavenumber k is given by $\Phi'(\varpi)$ and is negative for trailing spirals. Our definition differs from that used by Roberts (1969*a*) and Shu *et al.* (1972) essentially by a multiplicative factor $m/\sin i$, where $\tan i = -m/k\varpi$, and by an additive constant in η, chosen so that $\eta = 0$ describes asymptotically the locus of the *minimum* of the spiral potential. For fixed ϖ, note that one period, 2π, of ϕ corresponds to m periods, $m2\pi$, of η.

To lowest order for large $|k|\varpi$, i.e., for small sin i, the spiral gravitational field is directed in the η direction and has a maximum strength of

$$F = (k^2 + m^2\varpi^{-2})^{1/2}A/\varpi\Omega^2 \tag{4}$$

when expressed as a fraction of the axisymmetric field $\varpi\Omega^2 = \mathfrak{V}_0'(\varpi)$. In this paper we shall assume F not to be very large in comparison with sin i. We wish to express the steady gas dynamical equations in the (η, ξ) coordinates. Thus, we first resolve the fluid velocity vector into its η and ξ components:

$$u_\eta = u_{\eta 0} + u_{\eta 1}\,, \qquad u_\xi = u_{\xi 0} + u_{\xi 1}\,, \tag{5}$$

where the subscript 0 refers to the basic state and the subscript 1 refers to the perturbations. Along a streamline our position in the galaxy is given by the condition

$$\frac{d\xi}{d\eta} = \frac{(u_{\xi 0} + u_{\xi 1})}{(u_{\eta 0} + u_{\eta 1})}\,. \tag{6}$$

If we now keep only the lowest-order terms in the asymptotic approximation sin $i \ll 1$, the gas dynamical equations governing the perturbed flow read (cf. eqs. [9]–[11] of Roberts 1969*a*, or eqs. [30] of Shu *et al.* 1972):

$$(\sigma_0 + \sigma_1)(u_{\eta 0} + u_{\eta 1}) = \text{constant} \equiv \sigma_0 u_{\eta 0}\,, \tag{7a}$$

$$\frac{\partial u_{\eta 1}}{\partial \eta} = U(u_{\eta 0} + u_{\eta 1})\frac{(2u_{\xi 1} - F\varpi\Omega \sin \eta)}{(u_{\eta 0} + u_{\eta 1})^2 - a^2}\,, \tag{7b}$$

$$\frac{\partial u_{\xi 1}}{\partial \eta} = -V\frac{u_{\eta 1}}{(u_{\eta 0} + u_{\eta 1})}\,. \tag{7c}$$

[1] In this paper we shall not discuss the detailed relation between high gas compression and the process of star formation. The dependence of the rate of star formation on gas compression is highly sensitive to the model adopted for the structure of the interstellar medium on a small scale. The two-phase model of the interstellar medium (Pikel'ner 1967; Field, Goldsmith, and Habing 1969; Spitzer and Scott 1969) has accumulated considerable observational support (Hughes, Thompson, and Colvin 1971; Radhakhrishnan *et al.* 1972; Mebold 1972), and this is the model adopted in the calculations of Shu *et al.* (1972). These last-mentioned authors found the *large-scale dynamics* of the two-phase model to be very similar to the one-component isothermal model, but their picture for the compression of *individual interstellar clouds* is quite different. Somewhat different points of view on the problem of cloud formation in the two-phase model have been taken by Zel'dovich and Pikel'ner (1969) and Biermann *et al.* (1972).

In the above equations, $\sigma_0(\varpi)$ is a reference surface density; whereas $u_{\eta 0}$, $u_{\xi 0}$, U, and V are the velocity parameters

$$u_{\eta 0} = \varpi(\Omega - \Omega_p) \sin i\,, \qquad u_{\xi 0} = \varpi(\Omega - \Omega_p) \cos i\,, \tag{8a}$$

$$U = (m^{-1} \sin i)\varpi\Omega\,, \tag{8b}$$

$$V = (m^{-1} \sin i) \frac{d}{d\varpi} (\varpi^2\Omega) = (m^{-1} \sin i) \frac{\varpi\kappa^2}{2\Omega}\,. \tag{8c}$$

Of these, the parameter $u_{\eta 0}$ is especially significant since it corresponds to the component of the circular motion which is perpendicular to the wave front, $\varpi\Omega \sin i$, measured relative to the phase velocity of the background spiral density wave, $\omega/(k^2 + m^2\varpi^{-2})^{1/2} = \varpi\Omega_p \sin i$. Ignoring the minus sign, we shall henceforth refer to $u_{\eta 0}$ as the Doppler-shifted phase-velocity.

As long as F is not large in comparison with $\sin i$, we can regard $u_{\eta 0}$, $u_{\xi 0}$, U, and V to be constants when we integrate equations (7) along a streamline. In the order of approximation considered here, we may replace the requirement that the flow be single-valued in space by the requirement that the flow be periodic in η with period 2π.

Appendix D of Shu *et al.* (1972) shows that the effective acoustic speed a and the Doppler-shifted phase-velocity $u_{\eta 0}$ can generally be expected to have numerically similar values. On the other hand, $u_{\eta 0}$, U, and V are considered to be of the same order in the ordering scheme $\sin i \ll 1$; while $\varpi\Omega$, $\varpi\kappa^2/2\Omega$, and $u_{\xi 0}$ are considered to be one order larger. Clearly, if in addition F is assumed to be $O(\sin i)$, equations (7b) and (7c) would imply that $u_{\eta 1}$ and $u_{\xi 1}$ are of the same order as $u_{\eta 0}$, etc. By the same token, equation (7a) then implies that σ_1 is of the same order as the unperturbed density σ_0. *Thus, the density response of the interstellar gas is generally quite nonlinear even if the amplitude of the spiral gravitational field is only a small fraction of the unperturbed field.*

III. THE SLIGHTLY NONLINEAR REGIME

We begin our mathematical discussion with an analytical treatment of the slightly nonlinear regime which is similar to that given by Vandervoort (1971) and by Yuan (private communication).[2] For easy comparison with the results of the linear theory (cf. Lin, Yuan, and Shu 1969), we first define the dimensionless parameters

$$\nu \equiv m(\Omega_p - \Omega)/\kappa = -u_{\eta 0}/(2UV)^{1/2}\,, \tag{9a}$$

$$x \equiv (k^2 + m^2\varpi^{-2})a^2/\kappa^2 = a^2/2UV\,. \tag{9b}$$

If we further nondimensionalize the velocity variables

$$u \equiv u_{\eta 1}/(2UV)^{1/2}\,, \qquad v \equiv u_{\xi 1}/V\,, \tag{10}$$

we can write equations (7b) and (7c) in the dimensionless form

$$\frac{\partial u}{\partial \eta} = (-\nu + u) \frac{(v - f \sin \eta)}{(-\nu + u)^2 - x}\,, \qquad \frac{\partial v}{\partial \eta} = \frac{u}{(\nu - u)}\,, \tag{11}$$

[2] The analysis of Vandervoort is more involved than the discussion given here partly because he considers *self-sustained* density waves in the gaseous component while we ignore the self-gravity of the gas and merely compute its response to a given forcing function.

where f is the scaled field strength

$$f \equiv F\varpi\Omega/2V = \left(\frac{\Omega}{\kappa}\right)^2\left(\frac{mF}{\sin i}\right) . \tag{12}$$

For the parameter regime $f \ll 1$, we look for solutions of equation (11) in the form of series expansions in powers of f:

$$u = \sum_{s=1}^{\infty} f^s u_s , \qquad v = \sum_{s=1}^{\infty} f^s v_s . \tag{13}$$

The substitution of equations (13) into equations (11) yields the following set of equations which are to be solved successively for $u_1, v_1; u_2, v_2; \ldots$:

$$(\nu^2 - x)\frac{\partial u_1}{\partial \eta} + \nu v_1 = \nu \sin \eta , \qquad \nu \frac{\partial v_1}{\partial \eta} - u_1 = 0 ; \tag{14a}$$

$$(\nu^2 - x)\frac{\partial u_2}{\partial \eta} + \nu v_2 = 2\nu u_1 \frac{\partial u_1}{\partial \eta} + u_1(v_1 - \sin \eta) , \qquad \nu \frac{\partial v_2}{\partial \eta} - u_2 = u_1 \frac{\partial v_1}{\partial \eta} . \tag{14b}$$

$$\ldots$$

Consistent with equations (11), we may look for solutions periodic in η in which u is an even function of η and v is an odd function. In particular, equations (14) admit solutions in which the odd and even terms have the Fourier series expansion ($j = 1, 2, \ldots$):

$$u_{2j-1} = \sum_{l=1}^{j} \alpha_{2j-1,2l-1} \cos (2l - 1)\eta ,$$

$$v_{2j-1} = \sum_{l=1}^{j} \beta_{2j-1,2l-1} \sin (2l - 1)\eta , \tag{15a}$$

$$u_{2j} = \alpha_{2j,0} + \sum_{l=1}^{j} \alpha_{2j,2l} \cos 2l\eta , \qquad v_{2j} = \sum_{l=1}^{j} \beta_{2j,2l} \sin 2l\eta . \tag{15b}$$

The substitution of equations (15) into equations (14) results in the following successive expressions for the dimensionless Fourier coefficients (each of order unity):

$$\alpha_{11} = \nu(1 - \nu^2 + x)^{-1} , \qquad \beta_{11} = (1 - \nu^2 + x)^{-1} ; \tag{16a}$$

$$\alpha_{20} = -\tfrac{1}{2}\alpha_{11}\beta_{11} , \qquad \alpha_{22} = -\frac{\alpha_{11}\beta_{11}}{2}\left[\frac{1 + 2(\nu^2 + x)}{1 - 4(\nu^2 - x)}\right] ,$$

$$\beta_{22} = \frac{\beta_{11}^2}{2}\left[\frac{-3\nu^2 + x}{1 - 4(\nu^2 - x)}\right] . \tag{16b}$$

Note that the procedure given above fails at an infinite but countable number of points because of the presence of the "resonant denominators" in the coefficients (16). In general, the coefficients α_{ss} and β_{ss} become infinite at a radius where

$$\nu^2 - x = (u_{\eta 0}^2 - a^2)/2UV = n^{-2} , \qquad n = \pm s . \tag{17}$$

We adopt the sign convention of taking n negative when ν is negative (inside of corotation) and n positive when ν is positive (outside of corotation). Except for $n = \pm 1$,

we are dealing with ultraharmonic resonances since for $x = 0$ (i.e., zero pressure), they occur where the gas meets the wave at a frequency which is $1/n$ times the epicyclic frequency. Note that finite pressure shifts the $n = \pm 1$ resonances, the "Lindblad resonances," beyond the principal range, $-1 < \nu < 1$, where stellar density waves can propagate. For future reference, we also note that the resonance limits for $n \to \pm\infty$ occur where $u_{\eta 0} = \pm a$, i.e., where the basic flow is sonic. Moreover, whether the higher-harmonic response tends to reinforce or to interfere destructively with the fundamental response depends on whether we are on the high-frequency side, $\nu^2 > n^{-2} + x$, or on the low-frequency side, $\nu^2 < n^{-2} + x$, of the ultraharmonic resonance.

In the neighborhood of an ultraharmonic resonance, we require a more sophisticated treatment of the nonlinear gas dynamical equations. In § V, we shall take a numerical approach.[3]

When we are not near resonances, we may regroup equations (13) and (15) and write the solutions in terms of their various Fourier components:

$$u = A_0 + \sum_{s=1}^{\infty} A_s \cos s\eta\,, \qquad v = \sum_{s=1}^{\infty} B_s \sin s\eta\,. \tag{18}$$

The Fourier coefficients for the odd and even terms are given by ($l = 1, 2, 3, \ldots$)

$$A_0 = \sum_{j=1}^{\infty} f^{2j}\alpha_{2j,0}\,, \qquad A_{2l-1} = \sum_{j=l}^{\infty} f^{2j-1}\alpha_{2j-1,2l-1}\,, \qquad A_{2l} = \sum_{j=l}^{\infty} f^{2j}\alpha_{2j,2l}\,; \tag{19a}$$

$$B_{2l-1} = \sum_{j=l}^{\infty} f^{2j-1}\beta_{2j-1,2l-1}\,, \qquad B_{2l} = \sum_{j=l}^{\infty} f^{2j}\beta_{2j,2l}\,. \tag{19b}$$

Note that for $f \ll 1$, $A_0 = O(f^2)$, $A_s = O(f^s)$, $B_s = O(f^s)$. In particular, if we keep only terms of first order in f, we obtain $u_{\eta 1} = f(2UV)^{1/2}\alpha_{11}\cos\eta$ and $u_{\xi 1} = fV\beta_{11}\sin\eta$, which is asymptotically equivalent to the usual linear solution (see, e.g., eq. [2.17] of Lin *et al.* 1969).

For realistic amplitudes of the background forcing, f is of order unity so that the series (18) converges slowly, if at all. In particular, we shall see in § IV that a fundamental change in the solutions occurs when f exceeds a certain critical value which forces the flow to become transonic, i.e., which forces $(u_{\eta 0} + u_{\eta 1})$ to pass through the sound speed a. In such cases, the solutions for $u_{\eta 1}$ and $u_{\xi 1}$ lose their even and odd symmetry in η because a shift in phase is introduced by the production of galactic shocks.

IV. FULLY NONLINEAR WAVES AND THE INTRODUCTION OF SHOCKS

The dimensionless equations (11) contain three independent parameters—ν, x, and f—which measure, respectively, the intrinsic forcing frequency, the square of the acoustic speed, and the strength of the background spiral field. Clearly, an exhaustive numerical search for periodic solutions in all possible regions of this parameter space would be very time consuming; moreover, the significance of the results of such a search would not be easily assimilated.

In the rest of this paper we shall use the following procedure. We adopt a specific model for our own Galaxy—constructed in the manner outlined by Shu, Stachnik,

[3] A brief discussion of ultraharmonic and subharmonic resonances for self-sustained stellar density waves has been given by Contopoulos (1970). Kalnajs (as quoted by Simonson 1970) has considered ultraharmonic resonances for particles moving in purely circular orbits also from the standpoint of a series expansion of the perturbed motion.

TABLE 1

GALAXY PARAMETERS FOR A TWO-ARMED SPIRAL WAVE WITH $\Omega_p = 13.5$ km s^{-1} kpc^{-1}

ϖ (kpc) (1)	Ω (km s^{-1} kpc^{-1}) (2)	κ (km s^{-1} kpc^{-1}) (3)	i (degrees) (4)	$u_{\eta 0}$ (km s^{-1}) (5)	$u_{\xi 0}$ (km s^{-1}) (6)	U (km s^{-1}) (7)	V (km s^{-1}) (8)	$(u_{\eta 0}^2 - a^2)/2UV$ (for $a = 8$ km s^{-1}) (9)
4.0.....	52 6	86.1	7.2	19.5	155.0	13.1	17.6	0.685
5.0.....	45.5	74.5	7.3	20.4	158.6	14.5	19.5	0.623
6.0.....	40.1	63.8	7.0	19.5	158.4	14.7	18.6	0.577
7.0.....	35.5	54.0	6.7	18.0	153.2	14.5	16.8	0.534
8.0.....	31.5	45.2	6.6	16.4	143.0	14.4	14.8	0.483
9.0.....	27.9	37.5	6.5	14.7	128.6	14.3	12.9	0.415
10.0.....	24.7	31.0	6.7	13.0	111.2	14.4	11.3	0.326
10.5.....	23.2	28.2	6.8	12.1	101.6	14.5	10.6	0.271
11.0.....	21.9	25.6	7.0	11.2	91.6	14.6	10.0	0.211
11.5.....	20.6	23.3	7.2	10.2	81.3	14.8	9.4	0.145
12.0.....	19.4	21.2	7.4	9.2	70.7	15.0	8.9	0.075
12.5.....	18.3	19.4	7.6	8.0	60.0	15.2	8.5	0.003
13.0.....	17.3	17.7	7.9	6.8	49.3	15.5	8.1	−0.069
13.5.....	16.4	16.3	8.2	5.5	38.4	15.7	7.8	−0.138
14.0.....	15.5	15.0	8.4	4.1	27.7	15.9	7.5	−0.198
14.5.....	14.7	13.9	8.8	2.6	16.9	16.2	7.3	−0.242
15.0.....	13.9	12.9	9.2	1.0	6.3	16.6	7.1	−0.266

and Yost (1971)—whose velocity parameters $u_{\eta 0}$, U, and V as functions of the galactocentric radius ϖ are shown in columns (5), (7), and (8) of table 1. We shall calculate the streamline solutions at a variety of radii in the model, i.e., along one curve in the (ν, x)-plane, and hope that the conditions spanned will give a representative sample of the conditions likely to be encountered in other spiral galaxies.

To investigate the transition to transonic flow, we shall calculate the change in the behavior of the solution for a given streamline, i.e., with fixed ν and x, for different values of the background spiral field strength f. We can visualize this as a *development in time* only if we imagine a quasi-static process whereby we increase the value of f slowly enough that the flow at each value of f reached is described by the steady equations (11). To begin, we first consider a streamline with an average radius of 10 kpc.

a) Transition to Transonic Flow from Entirely Supersonic Flow

To keep closer to the physics, we shall describe the numerical solutions in terms of the dimensional variables and the dimensional equations (7). The parameter $u_{\eta 0}$ at $\varpi = 10$ kpc has the value 13.0 km s^{-1}. Hence, if we adopt a value 8 km s^{-1} for a, the flow at very small F must be entirely *supersonic*. In particular, for infinitesimal values of F, the results of § III show the periodic flow to describe a locus in the velocity plane which is a perfect ellipse:

$$\nu^{-2}\left(\frac{\kappa}{2\Omega}\right)^2(u_\eta - u_{\eta 0})^2 + (u_\xi - u_{\xi 0})^2 = \left[\frac{F\varpi\Omega}{2(1 - \nu^2 + x)}\right]^2 . \tag{20}$$

Numerical solutions of equations (7b) and (7c) bear out this qualitative behavior for small F. (The reader is referred to the Appendix for details on the techniques used to find the numerical solutions illustrated in this paper.)

For $F = 0.5$ percent, figure 1 shows a distortion of the ellipse, but no important qualitative difference emerges. For example, since equation (7a) implies that u_η is proportional to the specific area, σ^{-1}, the interstellar gas is compressed to the smallest volume at the location of the potential minimum, $\eta = 0$.

For $F = 0.90$ percent, the second harmonic in the periodic flow makes its presence felt strongly and introduces *two* velocity maxima, roughly at $\eta = \pm 90°$, in place of the single velocity maximum at $\eta = 180°$. This splitting of the density minimum occurs because we are just inside the $n^{-1} = -\frac{1}{2}$ ultraharmonic resonance at $\varpi = 10.7$ kpc (see col. [9] of table 1). Such splitting does not occur in the inner regions of the Galaxy.

Clearly, as F is increased further, the flow must eventually try to cross the sonic point, $u_\eta = a$, which is a singular point of equation (7b). Let the critical value of the field strength at which this first happens be denoted by $F_{\rm crit}$. In the Appendix we show that the flow for $F = F_{\rm crit}$ does not approach the sonic line, $u_\eta = a$, along a tangent in the velocity place. Instead the flow develops a cusp there. For this reason we henceforth denote $F_{\rm crit}$ by $F_{\rm cusp}$. Mathematically, the cusp arises because the sonic point is a *saddle point* of the system of differential equations (7b) and (7c) (Roberts 1969*b*; see also Butenin 1965). Physically, the cusp corresponds to a shock of zero strength.

Flow solutions with $F > F_{\rm cusp}$ are shown in figure 2. Each solution passes smoothly through one sonic point during the expansive part of the flow and forms a shock (for each period of η) of finite strength during the compressive part of the flow. At the same time, the location of the density maximum shifts upstream from the location of the potential minimum. This phase shift in the gaseous density response results in a net torque being exerted on the gas, the consequence of which is discussed in Roberts and Shu (1972; see also Kalnajs 1972). For the present we merely note that the shocks

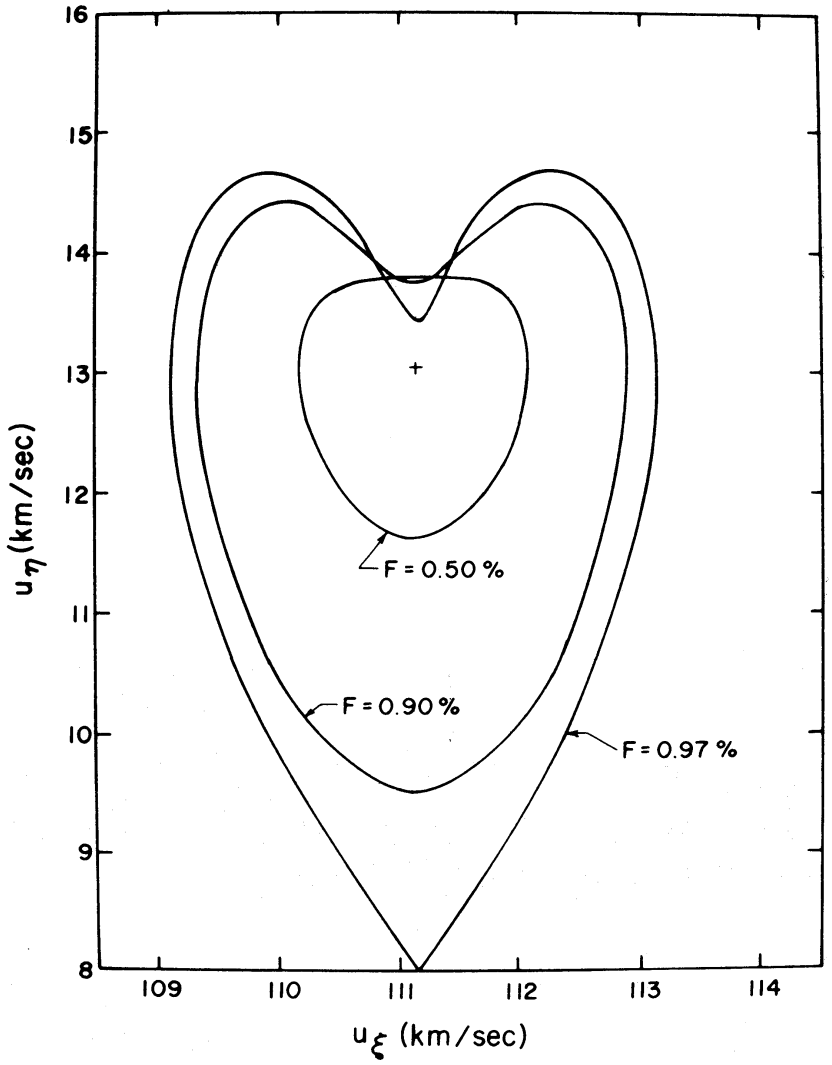

FIG. 1

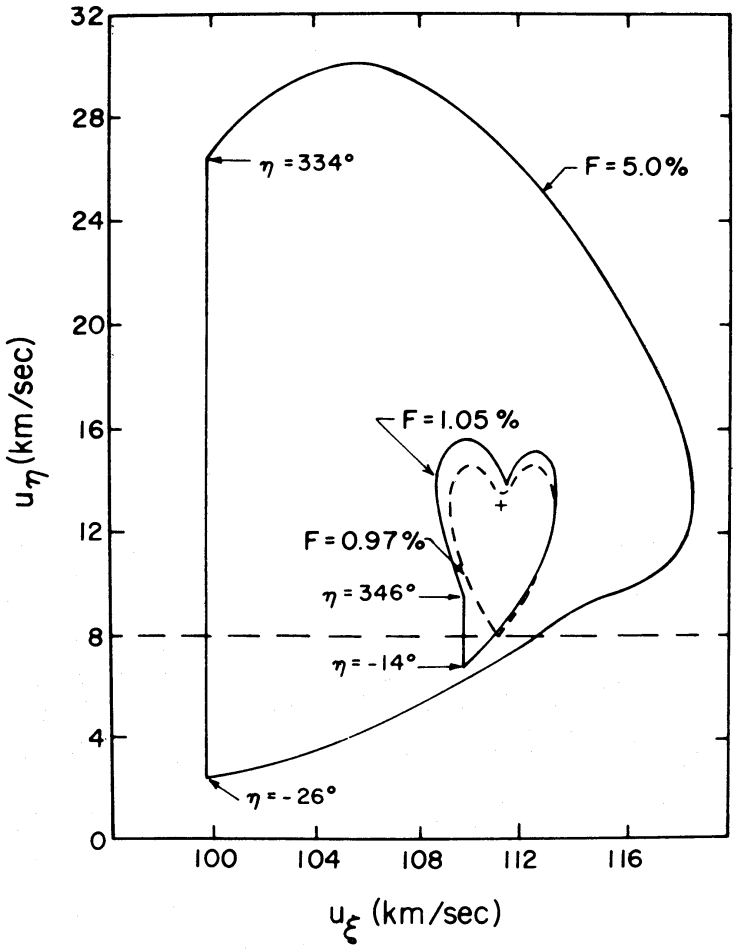

FIG. 2

FIG. 1.—Entirely supersonic flow in the velocity plane for $\varpi = 10$ kpc with $a = 8$ km s^{-1}. The unperturbed velocity is marked by a cross, and the flow proceeds in a counterclockwise direction. For $F = 0.97\%$, the flow contains a cusp at the location of the minimum of the spiral potential, $\eta = 0$.

FIG. 2.—Transonic flow in the velocity plane for $\varpi = 10$ kpc with $a = 8$ km s^{-1}. The unperturbed velocity is marked by a cross, and the flow proceeds in a counterclockwise direction. For $F > F_{\rm cusp} = 0.97\%$, the flow contains a shock located at the indicated value of η.

1973ApJ...183..819S

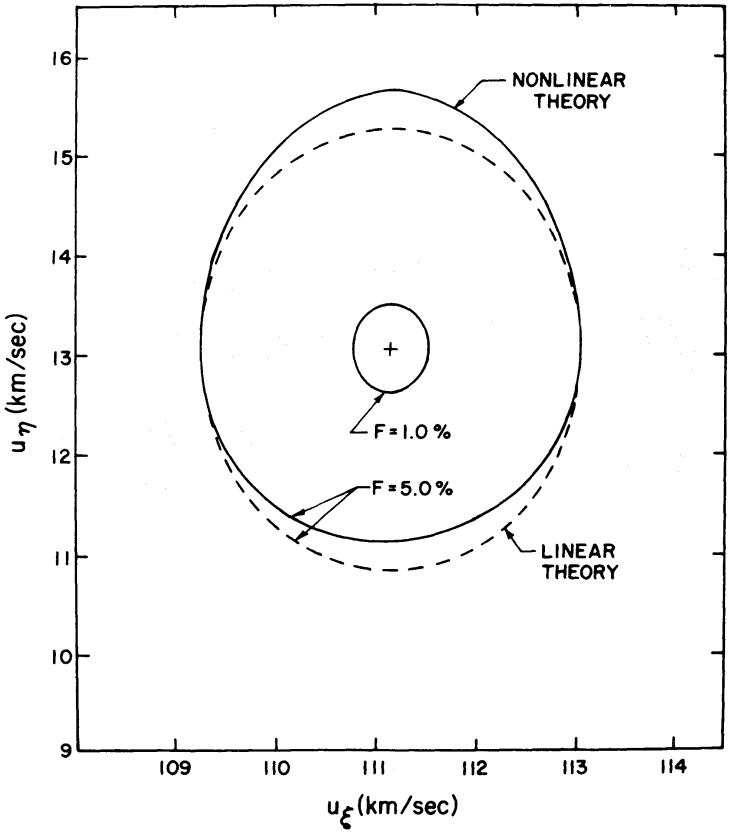

FIG. 3

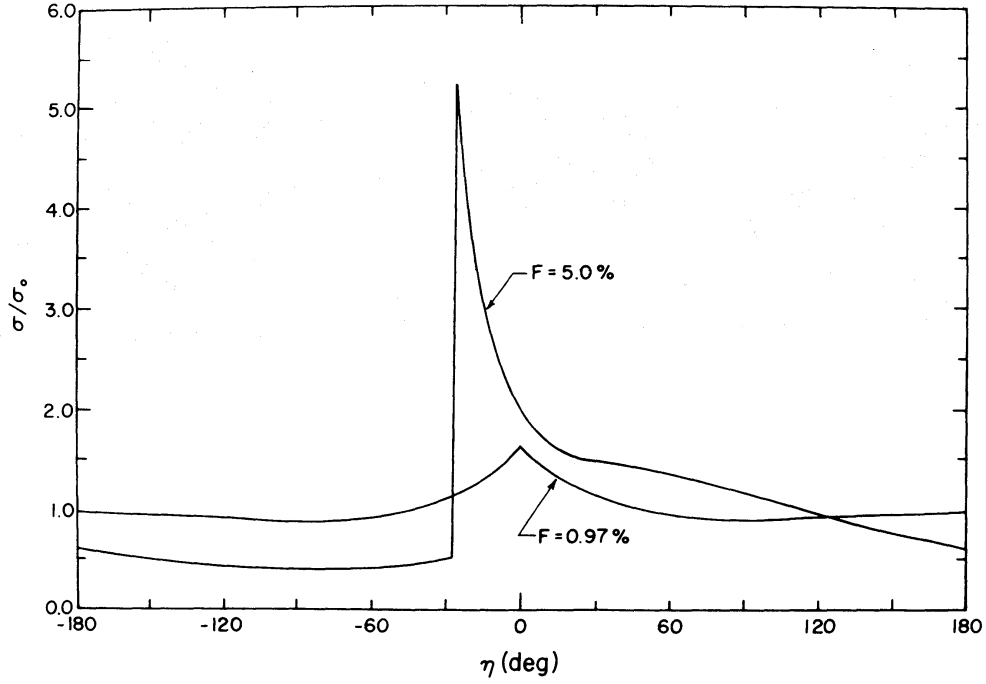

FIG. 4

FIG. 3.—Entirely subsonic flow in the velocity plane for $\varpi = 10$ kpc and $a = 30$ km s^{-1}. The solid curves are computed numerically from the nonlinear equations (7b) and (7c). The dashed curve gives the solution obtained from the linear theory.

FIG. 4.—The variation of the normalized density, σ/σ_0, as a function of the phase angle η for the flow at $\varpi = 10$ kpc with $a = 8$ km s^{-1}. The flow proceeds from left to right in the direction of increasing η. The spiral potential is given by $\mathfrak{V}_1 = -A \cos \eta$. Note that the solution for $F = 0.97\%$ contains a cusp at the location of the minimum of the spiral potential, $\eta = 0$.

develop because the spiral gravitational field forces gas moving at supersonic speeds to slam unknowingly into gas moving at subsonic speeds.

The crucial role played by a small value of a is illustrated in figure 3. Here the value of a adopted, 30 km s^{-1}, is typical of stellar dispersive speeds in the solar neighborhood. Clearly, in this case, even the response at $F = 5$ percent differs little from the behavior predicted by the linear theory.

The variation of the normalized gas density, σ/σ_0, is plotted in figure 4 as a function of η for the case $a = 8$ km s^{-1}. (In Roberts 1969, the corresponding figures are plotted as functions of η/m, whereas in Shu *et al.* 1972 they are plotted as functions of $\phi = \theta - \Omega_p t$.) For $F = 5$ percent, the value believed to be approximately present in the solar neighborhood (Yuan 1969), the shocks are quite strong and a factor 12:1 results for the total variation of the gas density. Moreover, the peak density reached is ~ 5 times larger than the average density, and the zone of high gas compression is confined to a very narrow spike. This behavior is characteristic for cases in which the

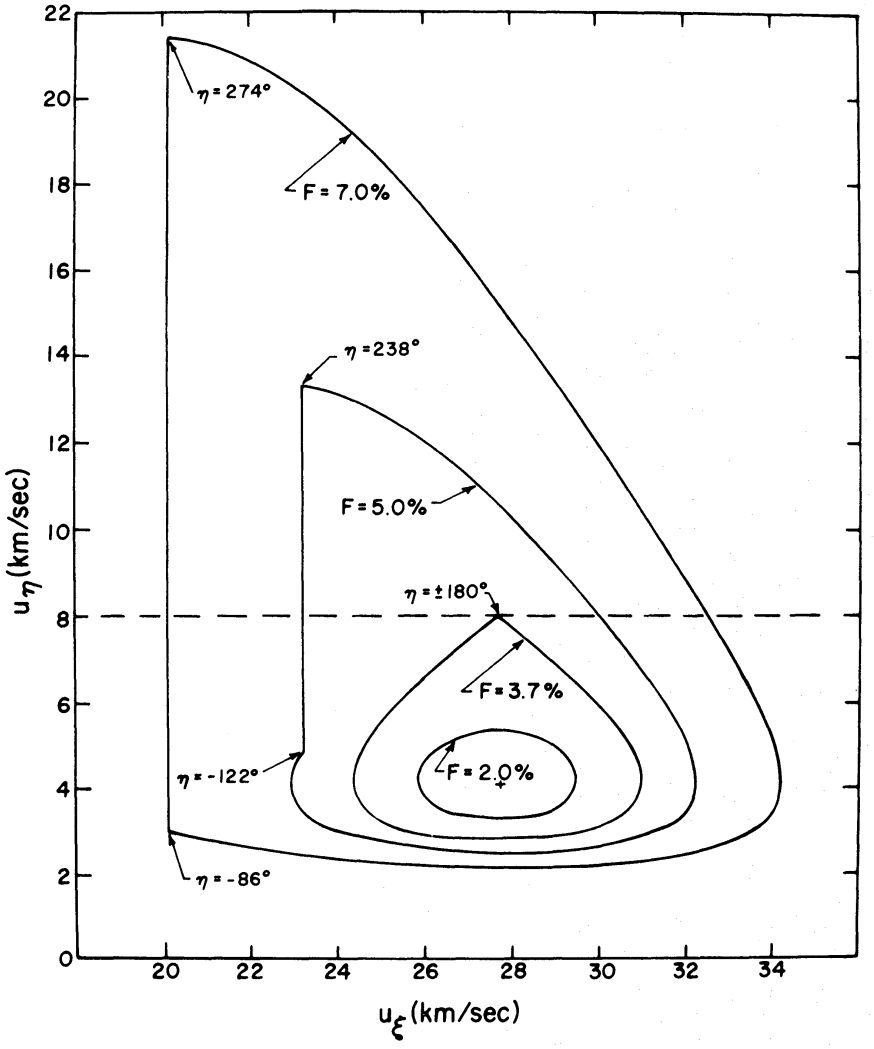

FIG. 5.—Flow in the velocity plane for $\varpi = 14$ kpc with $a = 8$ km s^{-1}. For $F < F_{\text{cusp}} = 3.7\%$, the flow is entirely subsonic. For $F > F_{\text{cusp}}$, the flow is transonic and contains a shock located at the indicated value of η.

basic flow is supersonic, i.e., for $u_{\eta 0} > a$. The situation when $u_{\eta 0} < a$ is investigated in the next subsection.

b) Transition to Transonic Flow from Entirely Subsonic Flow

Table 1 shows the parameter $u_{\eta 0}$ to decrease as we go outward from $\varpi = 10$ kpc. This happens because equation (8a) shows that $u_{\eta 0}$ must drop to zero as we approach the corotation radius, 15.3 kpc, where $\Omega = \Omega_p$. Thus, from 12.5 kpc to 15.3 kpc, $a > u_{\eta 0} > 0$; and the gas flow at small F is entirely *subsonic*.

Figure 5 shows the locus described by the flow in the velocity plane for a streamline with an average radius $\varpi = 14$ kpc. For $F = 2.0$ percent, there is only a slight distortion of the ellipse predicted by the linear theory. A cusp forms for $F = F_{\rm cusp} = 3.7$ percent. Note, though, that the cusp develops at the potential maximum, and that it corresponds to a density minimum. Thus, when F is increased beyond $F_{\rm cusp}$ and shocks of finite strength are produced, the shocks develop initially at the potential maximum and then move downstream in the direction of the potential minimum.

Plotted in figure 6 is the corresponding variation of the gas density as a function of η. Notice that the peak density is not reached immediately after the shock, but is attained subsequently by a *smooth* compression occurring at *subsonic* speeds. The zone of high gas compression is fairly broad—indeed, qualitatively, it is not unlike that produced by an extrapolation of the linear theory.

Clearly, if star formation were controlled essentially by the ambient gas pressure (which is proportional to the gas density in an isothermal model of the interstellar medium), the optical spiral arms defined by H II regions in this part of the Galaxy would be quite broad. Moreover, since the peak compression achieved is relatively

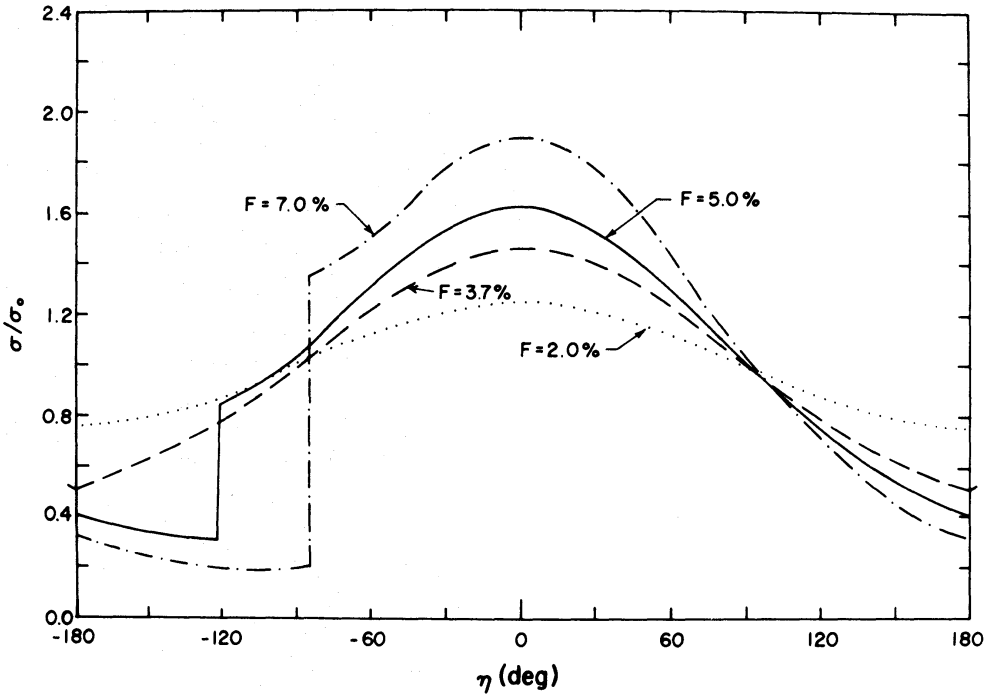

FIG. 6.—The variation of the normalized density, σ/σ_0, as a function of the phase angle η for the flow at $\varpi = 14$ kpc with $a = 8$ km s^{-1}. Note that the solution for $F = 3.7\%$ contains a cusp at the location of the maximum of the spiral potential, $\eta = \pm 180°$.

small, the number of H II regions would probably be small unless the strength of the spiral field were rather large (appreciably larger than, say, 7 percent).

We believe that the results of this subsection can be more profitably applied to explain the broad arms of a galaxy like M33, where $u_{\eta 0}$ is likely to have a small value throughout the disk (see fig. 6*a* of Shu *et al.* 1971). However, we should add the following qualifying remarks.

The solutions presented in figures 5 and 6 are not easy to find numerically by the iterative procedure outlined in the Appendix. Numerical integrations with slightly different starting values were often found to show very different behaviors from the "correct," i.e., periodic, solution. This apparent numerical instability may indicate a breakdown of the asymptotic approximation as we approach the singular point $u_\eta = 0$ of equation (7c). But it may also indicate that the nonlinear shock solutions found for $u_{\eta 0} < a$ are actually unstable physically.

Flows with shocks should satisfy the consistency relation that the shock front lie asymptotically close to an equipotential curve (see § VI*b* of Roberts 1972 and § III*f* of Shu *et al.* 1972). This consistency relation will not generally be satisfied when $u_{\eta 0} < a$ because the shock location along each streamline turns out to be a sensitive function of the parameters of the flow—especially of the parameter F. This difficulty could be removed by an appropriate *two-dimensional* integration of the steady gas-dynamical equations in which the location of the shock front is regarded as a free boundary.

On the other hand, the nonlinear solutions can be shown to be physically unstable only by including time dependence in the basic equations. Nonlinear time-dependent flows have been studied by Field and Woodward (private communication). For steady forcing conditions and $u_{\eta 0} > a$, they have obtained solutions which are very similar to those presented in the previous subsection. Of particular interest is their ability to follow the time-development of galactic shocks from the steepening of finite-amplitude waves, much as in the classical description by Riemann. As far as we are aware, Field and Woodward had not studied the case $u_{\eta 0} < a$ at the time of the writing of this paper.

V. ULTRAHARMONIC RESONANCES AND SECONDARY COMPRESSIONS

From equation (17) the response of the nth harmonic can be expected to be large whenever we are in the neighborhood of an ultraharmonic resonance where $(u_{\eta 0}^2 - a^2)/2UV = n^{-2}$. This is borne out by numerical calculations carried out for the range of radii from 10.0 kpc to 12.5 kpc in our adopted model (see table 1). On general principles, we can expect ultraharmonic effects to be most prominent in the neighborhood of 10.7 kpc in our model where $(u_{\eta 0}^2 - a^2)/2UV = (-\frac{1}{2})^2$.

Plotted in figures 7*a* and 7*b* for a variety of field strengths are the resulting flows for a streamline with average radius equal to 11 kpc. For $F = 0.5$ percent, we already begin to see a significant departure from the linear theory in the development of two lobes of gas compression. For $F = F_{\text{cusp}} = 1.1$ percent, the ends of these two lobes drop to touch the sonic line and introduce *two cusps* placed symmetrically about either side of the potential minimum. For $F > F_{\text{cusp}}$, the compressive parts of the flow ahead of each former cusp steepen to give shocks, but these shocks are of unequal strength. Apparently the formation of the first shock relieves the pressure head for the second shock.

The variation of the gas density as a function of η is plotted in figure 8. We believe that the second compression of the interstellar gas may generate secondary spiral features (cf. Roberts 1972) which appear downstream of the main shock (i.e., on the "outside" of the main spiral arm for $\Omega_p < \Omega$). In particular, the secondary compression associated with the $n^{-1} = -\frac{1}{2}$ resonance is found in our model to extend in

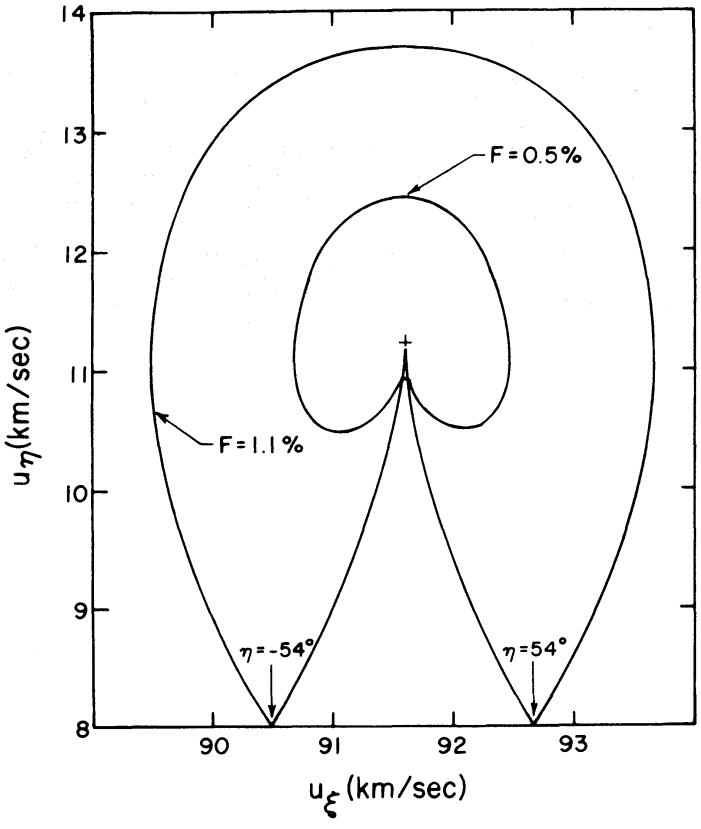

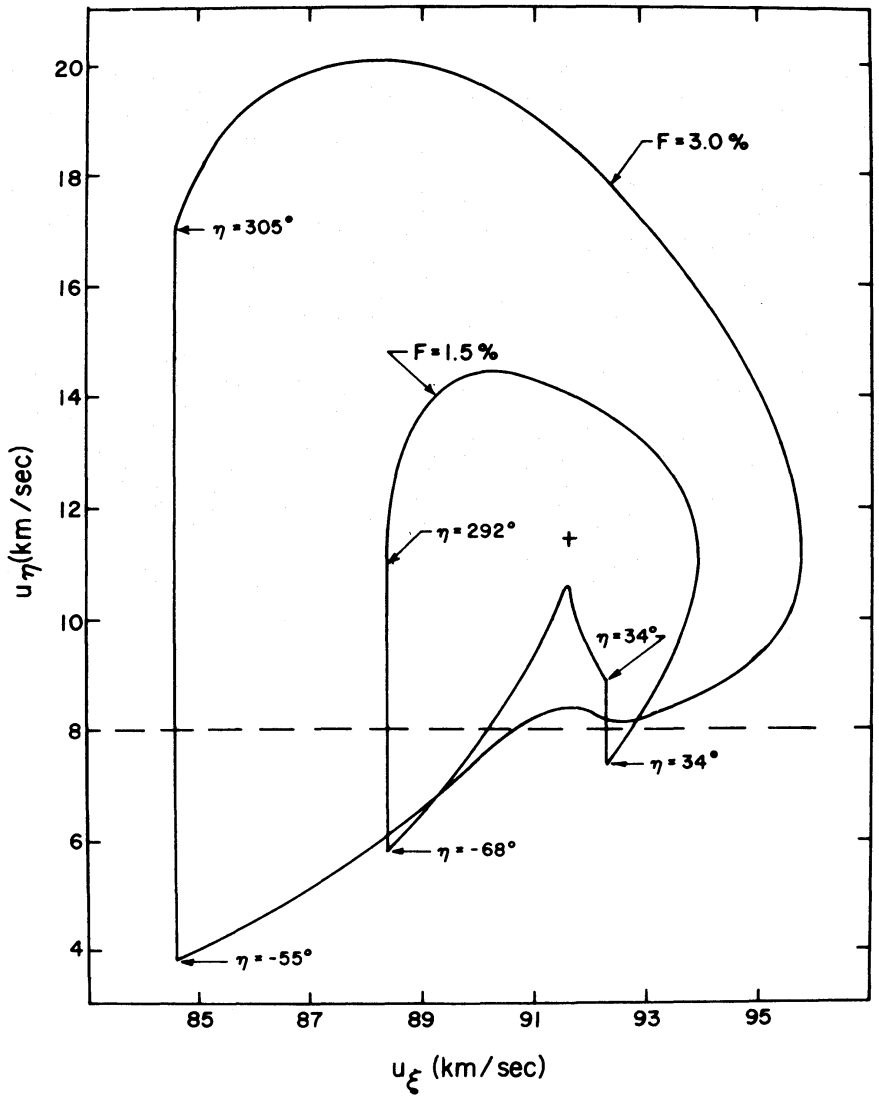

FIG. 7*a* (*left*).—Entirely supersonic flow in the velocity plane for $\varpi = 11$ kpc with $a = 8$ km s^{-1}. For $F = 1.1\%$, the flow contains two cusps located, respectively, at $\eta = \pm 54°$.

FIG. 7*b* (*right*).—Transonic flow in the velocity plane for $\varpi = 11$ kpc with $a = 8$ km s^{-1}. For $F > F_{\text{cusp}} = 1.1\%$, the flow contains two shocks located at the indicated values of η.

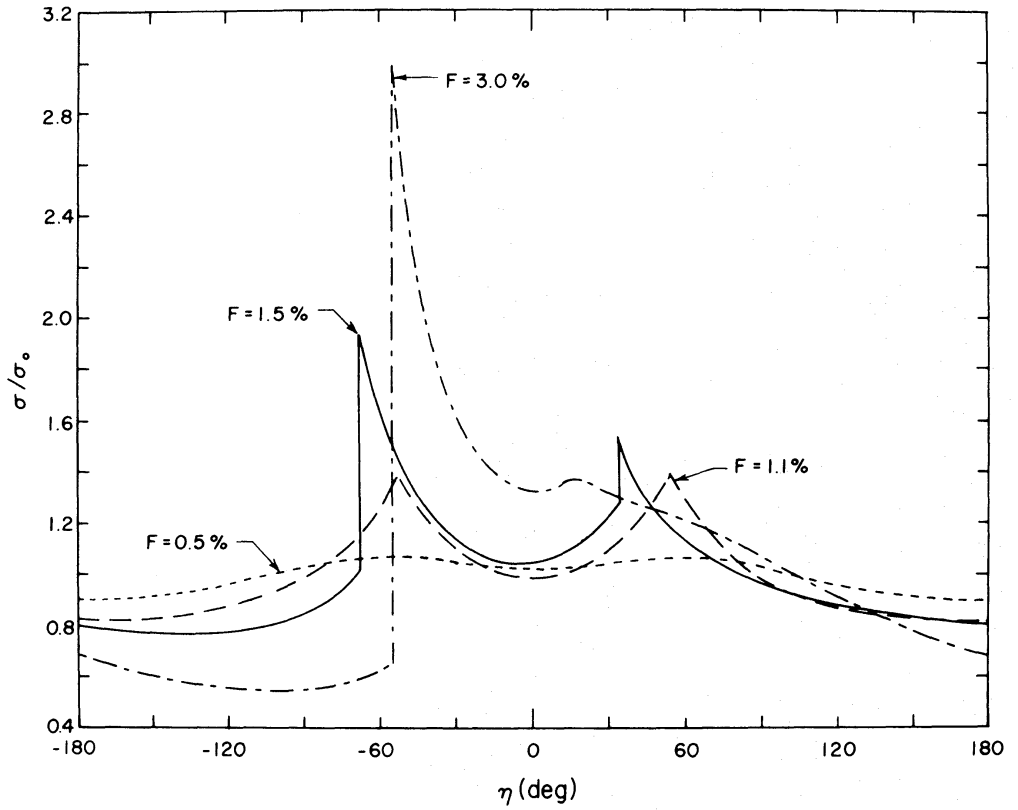

FIG. 8.—The variation of the normalized density, σ/σ_0, as a function of the phase angle η for the flow at $\varpi = 11$ kpc with $a = 8$ km s^{-1}. The secondary compression arises because the response is affected by the ultraharmonic resonance $n^{-1} = -\frac{1}{2}$.

radius from 10.6 kpc to 11.6 kpc and may well account for the origin of the Carina feature (see Bok 1971 and references therein). Note especially that the streaming velocity u_ξ on the inside edge of the secondary density concentration is smaller than that on the outside edge—just as is the case with the principal arms of a density wave (cf. Humphreys 1972). If the Carina spiral feature, and its radio counterpart on the opposite side of the Galaxy, owe their origin to this distinctly nonlinear effect, it would present a sensitive method to determine empirically an independent value for the pattern speed of the "grand design."

Figures 7 and 8 show the secondary shock to disappear when $F = 3$ percent at $\varpi = 11$ kpc. This suggests that the influence of the resonance is suppressed when the imposed forcing is sufficiently strong. In this connection, for the analysis near ultraharmonic resonances, it would be desirable to include the self-gravity of the gas. We should also not forget that concentrations of interstellar gas with masses characteristic of "spiral arms" can elicit very substantial responses in the stellar disk (Julian and Toomre 1966). *Thus, the gravitational potential associated with the secondary mass concentrations* (gaseous and stellar) *may well help to sustain them at considerably larger amplitudes than feasible by the simple sinusoidal forcing of the interstellar gas by a linear stellar density-wave.*

In comparison with the $n^{-1} = -\frac{1}{2}$ resonance, the $n^{-1} = -\frac{1}{3}, -\frac{1}{4}, \ldots$ resonances produce gaseous concentrations of considerably smaller radial extents. Thus, the higher-order ultraharmonic resonances may be capable of generating only relatively short spurs or feathers, and not major spiral features. Moreover, the "bootstrapping"

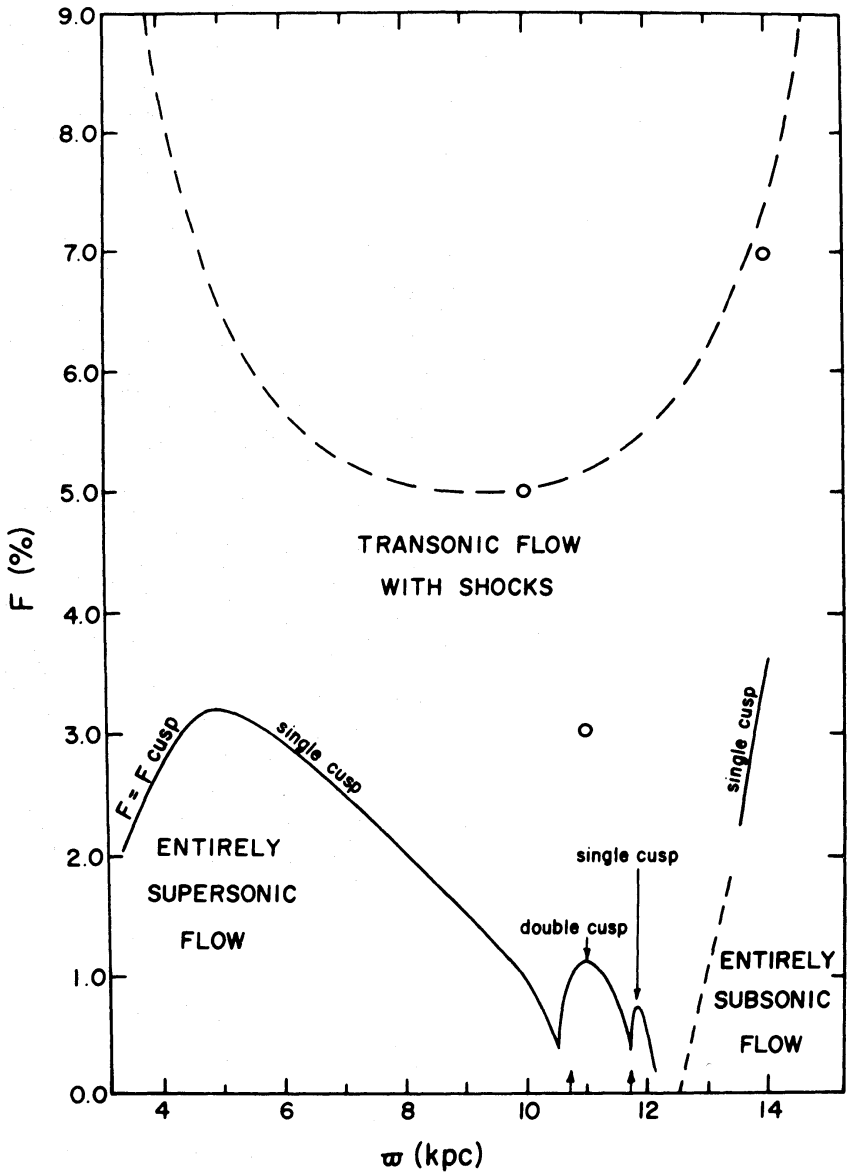

FIG. 9.—The field strength regime plotted as a function of the galactocentric radius ϖ in our model of the Galaxy. The left-hand border corresponds to the inner Lindblad resonance; the right-hand border, to the corotation radius. Solid line gives the value found for $F_{\rm cusp}$; the dashed line, the value of F implied by the amplitude relation of Shu when F is normalized to be 5.0% at $\varpi = 10$ kpc. For $F < F_{\rm cusp}$, the flow is entirely supersonic for $\varpi < 12.5$ kpc (where $u_{\eta 0} = a$), and is entirely subsonic for $\varpi > 12.5$ kpc. For $F > F_{\rm cusp}$, the flow is transonic and would necessarily contain shocks. The arrows on the abscissa at $\varpi = 10.7$ kpc and $\varpi = 11.7$ kpc mark the radii where $(u_{\eta 0} - a^2)/2UV$ equals, respectively, $(-\frac{1}{2})^2$ and $(-\frac{1}{3})^2$. The "cascade" which occurs for $F_{\rm cusp}$ as ϖ approaches the resonance limit, 12.5 kpc, is explained in the text. A numerical grid taken with 0.1-kpc spacing suffices to resolve only the ranges of the $-\frac{1}{2}$ and the $-\frac{1}{3}$ ultraharmonic resonances.

mechanism discussed above leads us to speculate that the resultant gas-star structures —in contrast to the indications of the purely gaseous response calculations—may have the large angles of inclination typical of real spurs and feathers (cf. fig. 11 of Julian and Toomre 1966). To be sure, our concentrations of gas are not orbiting at the circular speed of material clumps (modeled with *long-lived* mass points by Julian and Toomre), but the ray method of calculating steady patterns of waves produced by localized sources (Hunter 1972) suggests that the differences may not be great.

It has not been possible to study the flow for spiral field strengths much in excess of $F = 3$ percent at 11 kpc because shock solutions of the type considered in this paper cannot be found when the field strength exceeds a "cutoff" value (see Appendix). This obstacle arises because the one-dimensional nature of the asymptotic equations (7) places an overly restrictive condition on the sonic point in certain circumstances. We believe this difficulty to be an artificial one which may be removed by slightly relaxing the assumption that the properties of the flow vary only in the η-direction (perpendicular to spiral equipotentials).

We also note that the consistency requirement for asymptotic solutions containing galactic shocks mentioned in § IV*b* is not satisfied by our double-shock solutions. The locus of the secondary shock front is an especially sensitive function of the resonance parameter $(u_{\eta 0}^2 - a^2)/2UV = \nu^2 - x$, and does not in general coincide with an equipotential curve $\eta =$ constant. The above remarks coupled with those made at the end of § IV*b* indicate that a two-dimensional integration of the steady gas dynamical equations would be generally desirable for the outer parts of the galactic disk.

VI. SUMMARY

The main results of our numerical work are summarized in figure 9. In figure 9 we have plotted as a function of the galactocentric radius, the value of the field strength $F = F_{\text{cusp}}$ which barely gives rise to transonic flow in the model of our own Galaxy adopted in table 1.[4] For values of the field strength above F_{cusp}, the flow solutions develop shocks. For values of F below F_{cusp}, the flow solutions are everywhere smoothly varying.

The radius 10.7 kpc corresponds to an $n^{-1} = -\frac{1}{2}$ resonance; the radius 11.7 kpc, to an $n^{-1} = -\frac{1}{3}$ resonance; the radius 12.1 kpc, to an $n^{-1} = -\frac{1}{4}$ resonance; . . . ; and the radius 12.5 kpc, to the $n^{-1} = -1/\infty$ resonance limit (where $u_{\eta 0} = a$). The cusped solutions between 3.1 and 10.5 kpc contain one cusp; those between 10.5 and 11.7 kpc, two cusps; those between 11.7 and 12.1 kpc, one cusp; etc. This alternation between single-cusp solutions and double-cusp solutions generates a "cascade" of values of F_{cusp} which tend toward zero as we approach the resonance limit at 12.5 kpc. From 12.5 kpc to the corotation radius of 15.3 kpc, the basic flow is subsonic, $u_{\eta 0} < a$, and the cusped solution contains a single cusp located at the potential maximum rather than at the potential minimum.

We have plotted the values of F_{cusp} as a dashed line from 12.5 to 13.5 kpc because the "cutoff" described in the Appendix prevents us from obtaining cusped solutions for this range of radii. For base subsonic flow, $u_{\eta 0} < a$, the cutoff corresponds to a *lower* limit of F for which we can find periodic solutions that contain a sonic point. Thus, the cutoff does not prevent us from obtaining solutions which contain shocks of finite strength at larger F.

Also plotted in figure 9, as a dashed curve, is the field strength implied by the

[4] The inner Lindblad resonance in our model is at 3.1 kpc; the corotation radius, at 15.3 kpc. We have not tried to obtain solutions beyond the corotation radius because the physical conditions there are completely uncertain. However, for given values of f, U, and V, equations (7) show that solutions with $u_{\eta 0}$ and $u_{\xi 0}$ negative are easily generated formally from their counterparts with $u_{\eta 0}$ and $u_{\xi 0}$ positive by effecting the transformation $u_\eta \to -u_\eta$, $u_\xi \to -u_\xi$, and $\eta \to -\eta$.

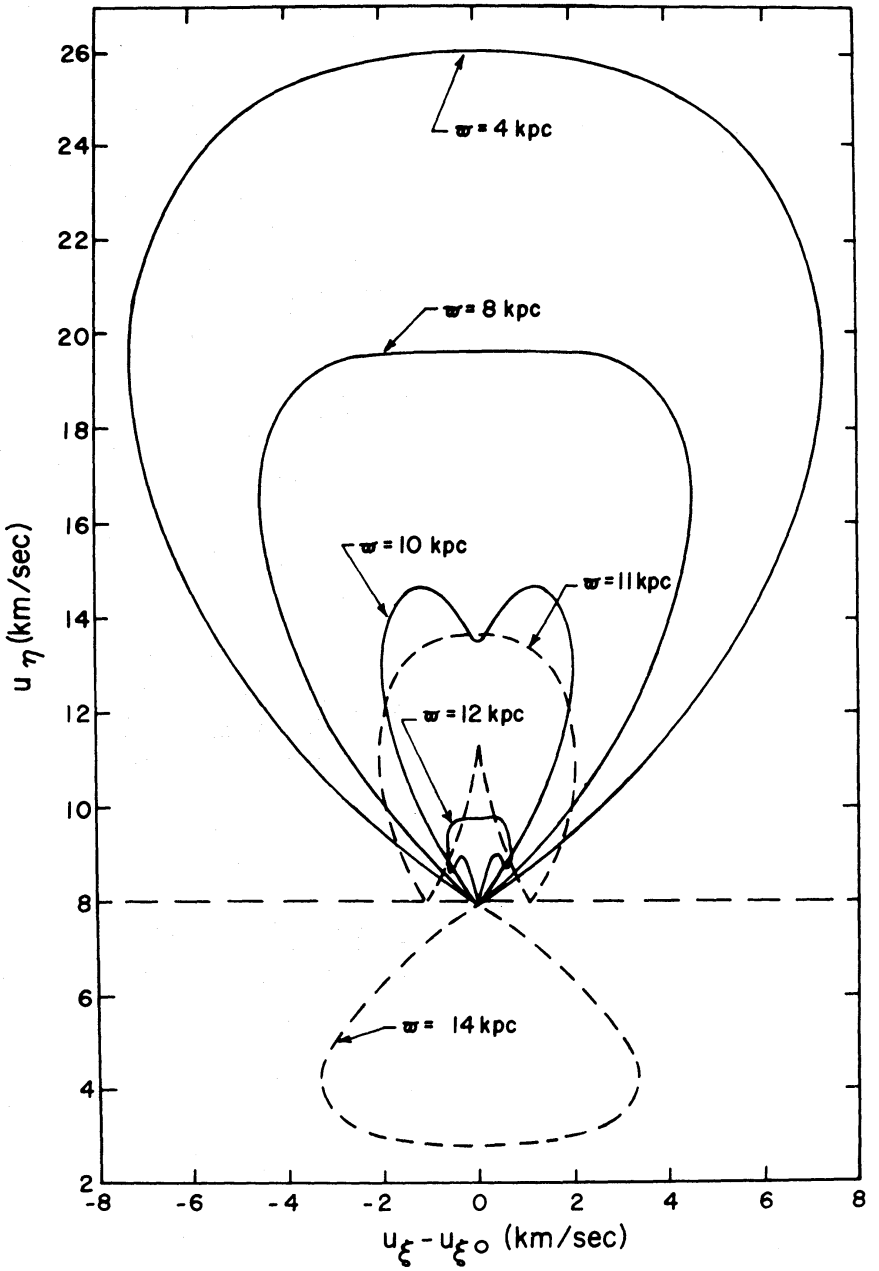

FIG. 10.—The character of the cusped solution as a function of the galactocentric radius ϖ in our model of the Galaxy. Although n local density maxima tend to be produced on the low-frequency side of the n^{-1} ultraharmonic resonance, only the largest of the local density maxima develops a cusp. For even n, two cusps form; for odd n, only one.

amplitude relation of Shu (1970)[5] when F is normalized to be 5 percent at $\varpi = 10$ kpc (Yuan 1969). Clearly if the distribution of the actual wave amplitude in the Galaxy were given by this curve, the gaseous response would be sufficiently strong to produce galactic shocks throughout the plotted regime. For reference, we have plotted the

[5] See also eq. (6a) of Shu *et al.* 1971; note, however, that eq. (6b) of Shu *et al.* 1971 contains a misprint: the minus sign should be contained outside the square brackets.

solutions of largest amplitude at each radius illustrated in this paper as unfilled circles in figure 9. The corresponding streamline solutions can be found in figures 2, 4, 5, 6, 7*b*, and 8.

The behavior of the cusped solutions in the velocity plane for various values of ϖ is illustrated in figure 10.[6] We see that n local density maxima tend to be produced on the low-frequency side of the n^{-1} resonance, but only the largest of these (there may be two equally large) would eventually form cusps. Thus, per period of η, we find that at larger F for n odd, only solutions with one shock are possible; whereas for n even, we can obtain solutions with two shocks. Note also that for $|n|$ larger than 2, there exists the possibility of minor compressions *both upstream and downstream* of the main shock.

Except for the $n^{-1} = -\frac{1}{2}$ ultraharmonic resonance, the additional compressive regions introduced by the influence of the ultraharmonic resonances may not persist for realistically large amplitudes of the forcing. Future studies of this point should include the effects of the "bootstrapping" mechanism which would be operative, as discussed in § V, in the presence of a responsive stellar disk. We suggest the lower-order members of the $n^{-1} = -\frac{1}{3}, -\frac{1}{4}, \ldots$ resonances to be definite candidates for further investigation as possible mechanisms for the production of the spurs and feathers which are often seen in the outer parts of external spiral galaxies. Looking ahead optimistically, one might even imagine using the ultraharmonic resonances observationally to study the mechanics of galaxies in a way analogous to the way that spectral lines are used to study the mechanics of atoms.

VII. DISCUSSION

In this paper, we have demonstrated that galactic shocks develop naturally, indeed *necessarily*, if the strength of the spiral gravitational field is larger than a certain critical value. By following this development numerically, we have ascertained that periodic shock solutions are simply the highly nonlinear members of a continuous family of solutions whose counterparts at infinitesimal amplitudes correspond to linear density waves.

We have also shown that the *breadth* of the zone of high gas compression is controlled by the relative magnitude of the Doppler-shifted phase-velocity $u_{\eta 0}$ compared to the effective speed of sound a. When $u_{\eta 0} > a$, as is likely in the interiors of galaxies exhibiting large differential rotation like our own Galaxy or M81, the zone of high gas compression is very narrow. When $u_{\eta 0} \lesssim a$, as is likely in galaxies which rotate almost uniformly like M33, the zone of high gas compression is broad. Galaxies of the latter type would also be more prone to the formation of secondary spiral features by the mechanism of ultraharmonic resonance. In such galaxies, the condition of near-resonance, $(u_{\eta 0}^2 - a^2)/2UV = \nu^2 - x \simeq (-\frac{1}{2})^2$, would be reached over a much wider range of radii. These trends can already be discerned from the results of Shu *et al.* (1971), but a more detailed discussion would be beyond the scope of the present paper.

We have not discussed in this paper why the spiral field should actually take on sufficiently large values to generate galactic shocks in the interstellar gas. Roberts and Shu (1972) have suggested that wave growth because of some as yet imperfectly

[6] The reader may well wonder how the cusped solutions at different radii are transformed continuously from one topology to another. Mathematically, additional lobes and cusps can be introduced after the flow forms loops in the velocity plane by passing through the unperturbed velocity point ($u_{\eta 1} = 0$, $u_{\xi 1} = 0$) which is a singular point of the system of differential equations (7b) and (7c). Physically, such contortions in the velocity plane, which do not manifest themselves quite so exotically in configuration space, arise because the character of the response of any mechanical system changes dramatically in the neighborhood of resonances.

understood mechanism of instability in the star-gas disk combined with the dissipation of such a wave by the development of galactic shocks may provide the limitation of the amplitude of the spiral field to some quasi-stationary value. This suggestion should be pursued further.

After this work was completed, we learned of an earlier independent study by Dr. Allan Saaf (1972) of the properties of slightly nonlinear density waves in the interstellar gas. Dr. Saaf's analysis is more general than the treatment given in § III since he does not use the approximation of small tilt angles. We wish to thank Dr. Saaf for sending us a preprint of his work. We also thank Professor C. C. Lin, Professor G. B. Field, Dr. C. Yuan, and Mr. P. Woodward for some stimulating discussions. We are grateful to Mr. Joel Bregman for computing assistance in the later stages of this work, and to the referee for some helpful suggestions for improving its presentation. The numerical calculations for this paper were performed at the Computing Center of Stony Brook. This work was supported in part by the National Science Foundation.

APPENDIX

We describe here the iterative numerical techniques used to find periodic solutions to equations (11). For entirely supersonic or entirely subsonic flows with given f, we integrate equations (11) step-by-step starting from $\eta = 0$ and ending at $\eta = 180°$. The solution for $0° \geq \eta \geq -180°$ is obtained from the requirement that u is even in η and v is odd. The starting value of v is, thus, zero at $\eta = 0$. The correct starting value of u at $\eta = 0$ must be chosen so that $v = 0$ at $\eta = \pm 180°$. We obtain the correct value by iteration with the initial guess guided by the analytical results of the perturbation series developed in § III.

If we increase f to some critical value $f_{\rm crit}$, the solutions not near ultraharmonic resonances begin to touch the sonic line. This occurs at the location $\eta = 0$ for transitions from entirely supersonic flow, i.e., when $\nu^2 > x$, and at the location $\eta = \pm 180°$ for transitions from entirely subsonic flow, i.e., when $\nu^2 < x$. For convenience of discussion, we define the dimensionless acoustic speed

$$\alpha = x^{1/2} = a/(2UV)^{1/2} . \tag{A1}$$

To be definite, consider the case $-\nu > \alpha$ (see fig. 1). For $f = f_{\rm crit}$, the most general solution of equations (11), which preserves the even and odd symmetry of u and v, and which is *continuous* in the neighborhood of the sonic point at $\eta = 0$, has the following series expansion:

$$u = (\alpha + \nu) + A|\eta| + \cdots, \qquad v = -\left(1 + \frac{\nu}{\alpha}\right)\eta - \frac{\nu}{2\alpha^2} A\eta^2 \,\text{sign}\,(\eta) + \cdots . \tag{A2}$$

In the above equation, the coefficient A is given by

$$A = (\tfrac{1}{2})^{1/2}[-(1 + \nu/\alpha) - f_{\rm crit}]^{1/2} , \tag{A3}$$

and is real and positive if $0 < f_{\rm crit} < -(1 + \nu/\alpha)$. Since the latter condition is found to be generally satisfied by the critical solution, equation (A2) implies the solution will generally contain a cusp at $\eta = 0$. For this reason, we denote the value of $f_{\rm crit}$ which leads to a periodic solution by $f_{\rm cusp}$. To find the numerical value of $f_{\rm cusp}$ we use the following procedure.

We make a guess for $f_{\rm crit}$ and obtain starting values at $\eta = 0^+$ by means of the series solution (A2). We then integrate equations (11) step-by-step to $\eta = 180°$. In

general the value of v reached at $\eta = 180°$ will not be zero. We continue to change $f_{\rm crit}$ by iteration until $v = 0$ at $\eta = 180°$. The solution for $0° \geq \eta \geq -180°$ is obtained by requiring that u is even in η and v is odd. Similar procedures are easily devised for the cases $-\nu < \alpha$ (subsonic flow inside of corotation), $\nu > \alpha$ (supersonic flow outside of corotation), and $\nu < \alpha$ (subsonic flow outside of corotation) (see also n. 4).

Significantly, the value of $f_{\rm cusp}$ determined in the above manner is found to be the *upper limit* of f for which we can find entirely supersonic (or entirely subsonic) flow solutions, and to be the *lower limit* of f for which we can find periodic shock solutions of the type described in § IV. This illustrates that the natural transition to transonic flow for $f > f_{\rm crit}$ cannot remain everywhere smooth by containing two symmetrically placed sonic points analogous to the hypothetical flows found for some periodic nozzles. Rather, the flow *must* develop shocks.

The procedure for finding the asymmetric single-shock solutions presented in § IV has been described, in the case of base supersonic flow, by Roberts (1969*b*) and in Appendix C of Shu *et al.* (1972). This procedure is trivially generalized to apply to the case of base subsonic flow.

In the neighborhood of ultraharmonic resonances corresponding to even values of n, two cusps can develop when f is increased to some critical value $f_{\rm cusp}$ (see fig. 7*a*). This trend can be followed from the formation of two lobes when the entirely supersonic solutions are pushed to values of f slightly less than $f_{\rm cusp}$. The two cusps are symmetrically located at $\eta = \pm\eta_c$. Our problem reduces to finding $f_{\rm cusp}$ and $\eta_c > 0$ which are not known *a priori*. We use the following procedure.

The series solution of equations (11) valid in the neighborhood of $\eta = \eta_c$ can be found as (for $-\nu > \alpha$)

$$u = (\alpha + \nu) + A_c|\eta - \eta_c| + \cdots,$$
$$v = f_{\rm cusp} \sin \eta_c - (1 + \nu/\alpha)(\eta - \eta_c) + \cdots, \tag{A4}$$

where the coefficient A_c is given by

$$A_c = (\tfrac{1}{2})^{1/2}[-(1 + \nu/\alpha) - f_{\rm cusp} \cos \eta_c]^{1/2}. \tag{A5}$$

We guess values for $f_{\rm cusp}$ and η_c and obtain starting values of u and v at $\eta = \eta_c{}^+$ and at $\eta = \eta_c{}^-$ by means of the series solution (A4). We integrate forward from $\eta = \eta_c{}^+$ to $\eta = 180°$ and integrate backward from $\eta = \eta_c{}^-$ to $\eta = 0$. We then check to see if v is zero both at $\eta = 0$ and at $\eta = 180°$. If not, we keep changing the guesses for $f_{\rm cusp}$ and η_c until v is zero at $\eta = 0$ and at $\eta = 180°$. An efficient iterative procedure for doing this is based on a two-dimensional analogue of Newton's method for finding roots. Finally, the flow for $0° \geq \eta \geq -180°$ is again obtained by imposing the even and odd symmetry of u and v.

If f is increased above $f_{\rm cusp}$ in the above case, two shocks will generally develop. The double-shock solutions are found by the following procedure. There are two sonic points $\eta = \eta_{A\rm SP}$ and $\eta = \eta_{B\rm SP}$, through which the flow passes *smoothly* by expanding from subsonic velocities to supersonic velocities. The series solution in the neighborhood of a sonic point $\eta_{\rm SP}$ has the appearance

$$u = (\alpha + \nu) + A_{\rm SP}(\eta - \eta_{\rm SP}) + \cdots,$$
$$v = f \sin \eta_{\rm SP} - (1 + \nu/\alpha)(\eta - \eta_{\rm SP}) + \cdots, \tag{A6}$$

where the coefficient $A_{\rm SP}$ is given by

$$A_{\rm SP} = (\tfrac{1}{2})^{1/2}[-(1 + \nu/\alpha) - f \cos \eta_{\rm SP}]^{1/2}. \tag{A7}$$

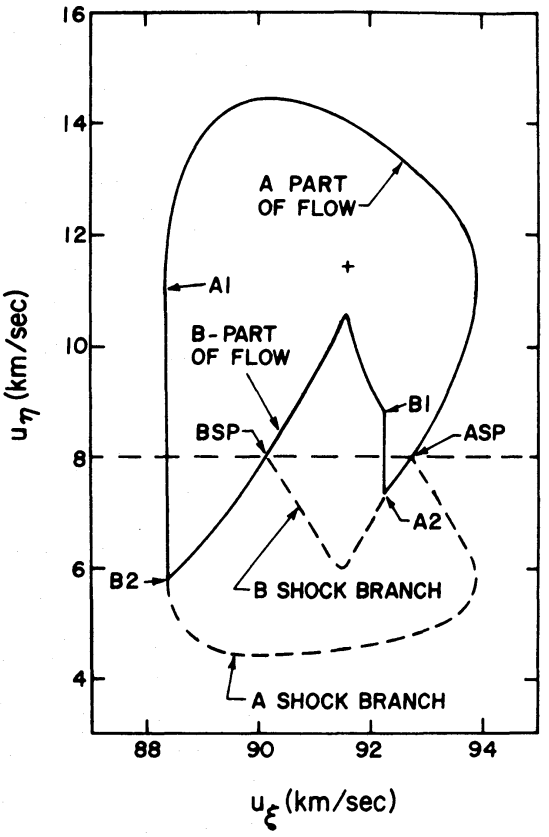

FIG. 11.—The procedure used to obtain a double-shock solution. The example shown corresponds to $\varpi = 11$ kpc, $a = 8$ km s^{-1}, and $F = 1.5\%$. Explanation for the various labels is given in the Appendix.

For given $f > f_{\rm cusp}$, we guess values for η_{ASP} and η_{BSP}. For each value of η_{SP}, we integrate forward in η to find the (A or B) supersonic branch of the flow, and backward in η to find the (A or B) subsonic branch (see fig. 11). For each point η on the A and B supersonic branches, we simultaneously compute the jump which would result were the flow to shock at that point. If we denote the flow immediately upstream of the shock by "1" and immediately downstream by "2," we have the jump conditions for an isothermal shock:

$$[-v + u(2)] = \alpha^2/[-v + u(1)]\,, \qquad v(2) = v(1)\,. \tag{A8}$$

The intersection $B2$ in the velocity plane of the hypothetical A shock-branch with the B subsonic-branch gives a possible shock. Similarly, the intersection $A2$ of the hypothetical B shock-branch with the A subsonic-branch gives another possible shock. However, these shocks will not arise unless the flows refer to the same point in η-space. Thus, we require

$$\eta(B1) - \eta(A2) = 0 \qquad \text{and} \qquad \eta(A1) - \eta(B2) = 360^\circ \tag{A9}$$

at the two shocks. Conditions (A9) will generally not be satisfied unless η_{ASP} and η_{BSP} are chosen properly. For given $f > f_{\rm cusp}$, the correct choice of η_{ASP} and η_{BSP} can again be found by an iterative procedure based on a two-dimensional analogue of Newton's method for finding roots. Four-place accuracy is easily achieved.

In summary, we remark that our experience shows each of the solutions described above is uniquely specified by (ν, x, f). The only problem which can arise is the possibility that for given f we can find *no* location of the sonic point η_{SP} which produces a periodic solution containing shocks. This can occur because the assumption that the flow varies only in the η-direction places a condition (i.e., eq. [A6]) on the sonic point analogous to the requirement of a "throat" in nozzle flow. The coefficient A_{SP} in equation (A7) is real only if the field strength f and the location η_{SP} of the sonic point are restricted to values which satisfy the inequality

$$-1 + |\nu|/\alpha - f\cos\eta_{SP} > 0\,. \tag{A10}$$

As a general rule, the location of the sonic point is such that $\cos(\eta_{SP}) > 0$ for $|\nu| > \alpha$, and $\cos(\eta_{SP}) < 0$ for $|\nu| < \alpha$. Thus, cutoff on the possible values of f can occur either as an upper limit if $|\nu| > \alpha$, or as a lower limit if $|\nu| < \alpha$. These facts can be stated quantitatively by noting that inequality (A10) implies that

$$f < (|\nu|/\alpha - 1)/\cos\eta_{SP} \qquad \text{if } \cos\eta_{SP} > 0\,,$$

and that

$$f > (1 - |\nu|/\alpha)/|\cos\eta_{SP}| \qquad \text{if } \cos\eta_{SP} < 0\,.$$

REFERENCES

Biermann, P., Kippenhahn, R., Tscharnuter, W., and Yorke, H. 1972, *Astr. and Ap.*, **19**, 113.
Bok, B. J. 1971, in *Highlights in Astronomy*, **2**, 66.
Butenin, N. V. 1965, *Elements of the Theory of Nonlinear Oscillations* (New York: Blaisdell).
Contopoulos, G. 1970, *Ap. J.*, **160**, 113.
Field, G. B., Goldsmith, D. W., and Habing, H. J. 1969, *Ap. J. (Letters)*, **155**, L149.
Fujimoto, M. 1966, in *IAU Symposium No. 29*, p. 453.
Goldreich, P., and Lynden-Bell, D. 1965, *M.N.R.A.S.*, **130**, 125.
Hughes, M. P., Thompson, A. R., and Colvin, R. S. 1971, *Ap. J. Suppl.*, **23**, 323.
Humphreys, R. M. 1972, *Astr. and Ap.*, **20**, 29.
Hunter, C. 1973, *Ap. J.*, **181**, 685.
Julian, W. H., and Toomre, A. 1966, *Ap. J.*, **146**, 810.
Kalnajs, A. J. 1972, *Ap. Letters*, **11**, 41.
Lin, C. C. 1971, in *Highlights of Astronomy*, **2**, 88.
Lin, C. C., Yuan, C., and Shu, F. H. 1969, *Ap. J.*, **155**, 721.
Mathewson, D. S., Kruit, P. C. van der, and Brouw, W. N. 1972, *Astr. and Ap.*, **17**, 468.
Mebold, U. 1972, *Astr. and Ap.*, **19**, 13.
Piddington, J. H. 1973, *Ap. J.*, **179**, 755.
Pikel'ner, S. 1967, *Astr. Zh.*, **44**, 1915.
Radhakhrishnan, V., Murray, J. D., Lockhart, P., and Whittle, R. P. J. 1972, *Ap. J. Suppl.*, **24**, 15.
Roberts, W. W. 1969*a*, *Ap. J.*, **158**, 123.
———. 1969*b*, Ph.D. thesis, MIT.
———. 1972, *Ap. J.*, **173**, 259.
Roberts, W. W., and Shu, F. H. 1972, *Ap. Letters*, **12**, 49.
Roberts, W. W., and Yuan, C. 1970, *Ap. J.*, **161**, 887.
Saaf, A. F. 1972, abstract in *Bull. A.A.S.*, **4**, 315; full-length paper to be submitted.
Shu, F. H. 1970, *Ap. J.*, **160**, 99.
Shu, F. H., Stachnik, R. V., and Yost, J. C. 1971, *Ap. J.*, **166**, 465.
Shu, F. H., Milione, V., Gebel, W., Yuan, C., Goldsmith, D. W., and Roberts, W. W. 1972, *Ap. J.*, **173**, 557.
Simonson, S. C. 1970, *Astr. and Ap.*, **9**, 163.
Spitzer, L., and Scott, E. H. 1969, *Ap. J.*, **158**, 161.
Vandervoort, P. O. 1971, *Ap. J.*, **166**, 37.
Yuan, C. 1969, *Ap. J.*, **158**, 889.
Zel'dovich, Ya. B., and Pikel'ner, S. B. 1969, *Zh. Eskeper. i Teoret. Fiz.*, **56**, 310.